Electronic Supplementary Material (ESI) for RSC Advances.

Seed treatment with iron pyrite (FeS_2) nanoparticles increase the production of spinach

Gaurav Srivastava[1*], Chinmaya Kumar Das[1], Anubhav Das[1], Satish Kumar Singh[2], Manas Roy[3], Hansung Kim[4], Niroj Sethy[5], Ashok Kumar[6], Raj Kishore Sharma[7], Sushil Kumar Singh[8], Deepu Philip[9,10], Mainak Das[1,10*]

[1] Bioelectricity, Green Energy, Physiology & Sensor Group, Laboratory XII, Department of Biological Sciences and Bioengineering, Indian Institute of Technology Kanpur, Kanpur, Uttar Pradesh, PIN 208016, India

[2] Institute Nursery, Indian Institute of Technology Kanpur, Kanpur, Uttar Pradesh, PIN 208016, India

[3] Department of Chemistry, Lovely Professional University, Phagwara, Punjab, 144411, India

[4] Department of Chemical & Biomolecular Engineering, Yonsei University, 134 Sinchon-dong, Seodaemon-gu, Seoul, 120-749, South Korea

[5] Defense Institute of Physiology & Allied Sciences, Defense Research Development Organization, Government of India, Timarpur, Delhi, PIN 110054, India

[6] Department of Biological Sciences and Bioengineering, Indian Institute of Technology Kanpur, Kanpur, Uttar Pradesh, PIN 208016, India

[7] Electrochemical Materials Research Group, Division of Physical Chemistry, Department of Chemistry, Delhi University, Delhi, PIN 110007, India

[8] Functional Materials Division, Solid State Physics Laboratory, Defense Research Development Organization, Government of India, Timarpur, Delhi, PIN 110054, India

[9] Industrial & Management Engineering, Indian Institute of Technology Kanpur, Kanpur, Uttar Pradesh, PIN 208016, India

[10] Design Program, Indian Institute of Technology Kanpur, Kanpur, Uttar Pradesh, PIN 208016, India

GS and MD are co-corresponding authors. Correspondence and requests for materials should be addressed to M.D. Email: mainakd@iitk.ac.in

Supplementary Information

Section S1

Seed Treatment Route	Species of Plant	Methodology	Results
Chemical Treatment (References)			
Brassins: steroid plant hormone[1]	Barley	1 minute soaking in methylene chloride with 100ppm brassin	Accelerated leaf growth and plant height.
Sulphuric acid, Nitric acid, hot water and sodium hypochlorite[2]	Acacia	5 and 10 minute treatment	Earlier germination and higher germination percentage. Maximum in Sulphuric acid treatments.
KNO_3 [3]	Himalayan oak	Pre soaking with 1% solution	Increased germination percentage from 56.7 % (control) to 81.1 % (test)
Thio urea [4, 5]	Lettuce	$3*10^{-2}$M	Stimulate germination
Kinetins [4]	Lettuce	10^{-5}M	Stimulate germination and enhance mitotic activity
Gibberellins [4, 5]	Lettuce	$3*10^{-4}$M + far red light	Stimulate germination
Biogas fermentative liquid[6]	Rice	Pre-soaking	Enhanced germination and yield.
Ehtylene [5]	Lettuce	10 µl/l treatment, + red light treatment	High increase (upto 40%) in germination
Physical Treatment			
Magnetic field [7]	Lentil	0.18T to 0.24 T for 20 minutes	Upto 33% increase in germination.
Microwaves [8]	Wheat	20 minutes treatment with 30 GHz waves	Improvement in germination percentage,height of seedling and length of root.
Scarification [3]	Himalayan oak	Cut at the chalazal end	Increased germination percentage from 56.7 % (control) to 94.4 % (test)
Sonication [9, 10]	Switch grass	22 min., 39C, 348W	Greater germination percentage and seedling growth
	Barley	5,10,15 min, 460W	Greater germination percentage and increased amylase activity
Photo treatment [4]	Lettuce	1 and 57 microwatts/mm^2 of radiant energy under the red and the far-red filter systems, respectively.	Increased germination
Temperature [11]	Locust bean tree	Treatment with boiling water for 5 seconds	Higher germination percentage
Soaking [12]	Teak	Soaking in running water for 24 hours	Significant increase in germination, no. of leaves, seedling height and shoot/root ratio
Nanoparticle Treatment			
Soaking in FeS2 nanoparticle + Water [13]	Cicer aritenum	Soaking for 14-16 hours	Significant increase in biomass of the plants grown for 7 days in the laboratory condition

Table S1. Summary of various chemical and physical seed treatment agents that enhance plant growth. Further recent studies have shown that molecules like H_2O_2, which were previously considered as damaging molecules for plant growth, exhibit germination enhancement properties, when seeds are incubated in low concentrations of H_2O_2[14-17].

Section S2

Effect of different kinds of nanomaterials (iron pyrite, cerium oxide and graphene oxide), salts (Fe, Ce) and charcoal on seed emergence:

This experiment was performed to verify whether all types of nanomaterials or only certain specific type of nanomaterials exhibit growth promoting effects upon seed treatment. The results are summarized in Figure S1a. Similarly, we explored whether the corresponding iron salt, cerium salt, and charcoal exhibit any plant growth promoting effects or not. This experimental result formed the basis from which iron pyrite nanoparticles were selected for field trial. The results are summarized in Figure S1b.

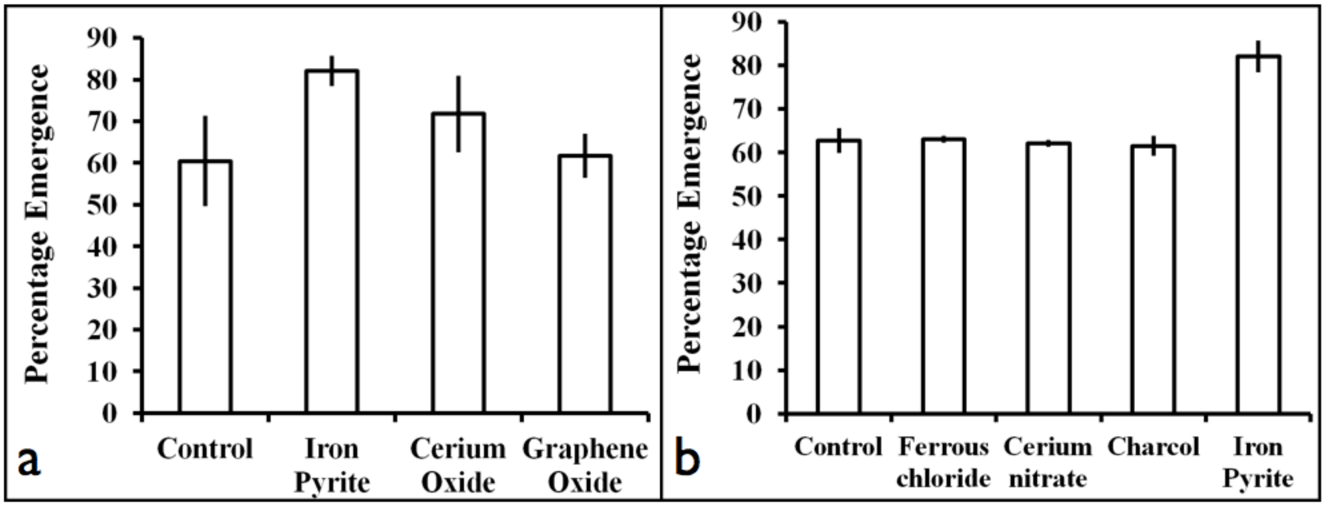

Figure S1. Effect of various nanomaterials (CeO, FeS_2, Graphene oxide), salts (Fe and Ce) and charcoal on seed emergence was observed. These experiments were repeated 6 times (n=6) and the results are expressed in mean ± standard error. **a.** Effects of different nanomateials. Significantly high emergence was observed in iron pyrite (82.11 ± 3.16) treated seeds as compared to control (60.44 ± 10.33). Cerium oxide (71.77 ± 8.66) also shows an increase in emergence while graphene oxide (61.66 ± 4.81) shows no difference with respect to control. **b.** Effect of different salts of iron (Fe), cerium (Ce) and charcoal on seed emergence and compared with iron pyrite nanoparticles. Both ferrous chloride (63.03 ± 0.30), cerium nitrate (62.12 ± 0.30) salts and charcoal (61.51 ± 1.84) showed no significant difference with respect to control (62.72 ± 2.40), whereas iron pyrite nanoparticles (82.11 ± 3.16) shows highly significant increase in emergence.

Experimental methods:

Emergence study: 1 gram of spinach seeds were taken in petriplates. Seeds were sterilized with 10% sodium hypochlorite for 10 minutes and washed thoroughly with distilled water. Control seeds were suspended in 20ml distilled water. Test seeds were also suspended in equal amount of nanomaterial suspension (100µg/ml). All nanomaterial suspensions were sonicated for 30 minutes at 53 kHz. The seeds were primed for 14 hours and the leachate was collected for further analysis. Then the seeds were kept moist by using layers of tissue paper. Count for total emergence was done on 7th day after removal of the lechate. Similar procedure was repeated to study the effect of various salts on seed emergence.

Synthesis and characterization of cerium oxide nanoparticles:

Cerium oxide nanoparticles were synthesized as described by us in our earlier publications[18,19]. Briefly, equal volume (100ml) 0.025 M solution of Cerium nitrate hexahydrate and 0.025 M solution of Hexa methylene-tetra-amine (HMTA) were mixed and maintained at 75-80°C in a water bath. Initial turbidity was observed, and as the time progressed, the solution slowly turned purple pink in color. As heating continued, the color of the solution changed to white, following which a turbid solution was obtained finally. Heating was done for 3 hours. The solution was centrifuged at 10000 rpm for a duration of 5 minutes. The precipitate was washed with acetone and water and the supernatant was discarded. The final precipitate was vacuum dried and further characterized. The particles used for the study were characterized by TEM and XRD analysis. These particles were smaller then the FeS_2 particles and exhibited more or less a spherical geometry (Figure S3).

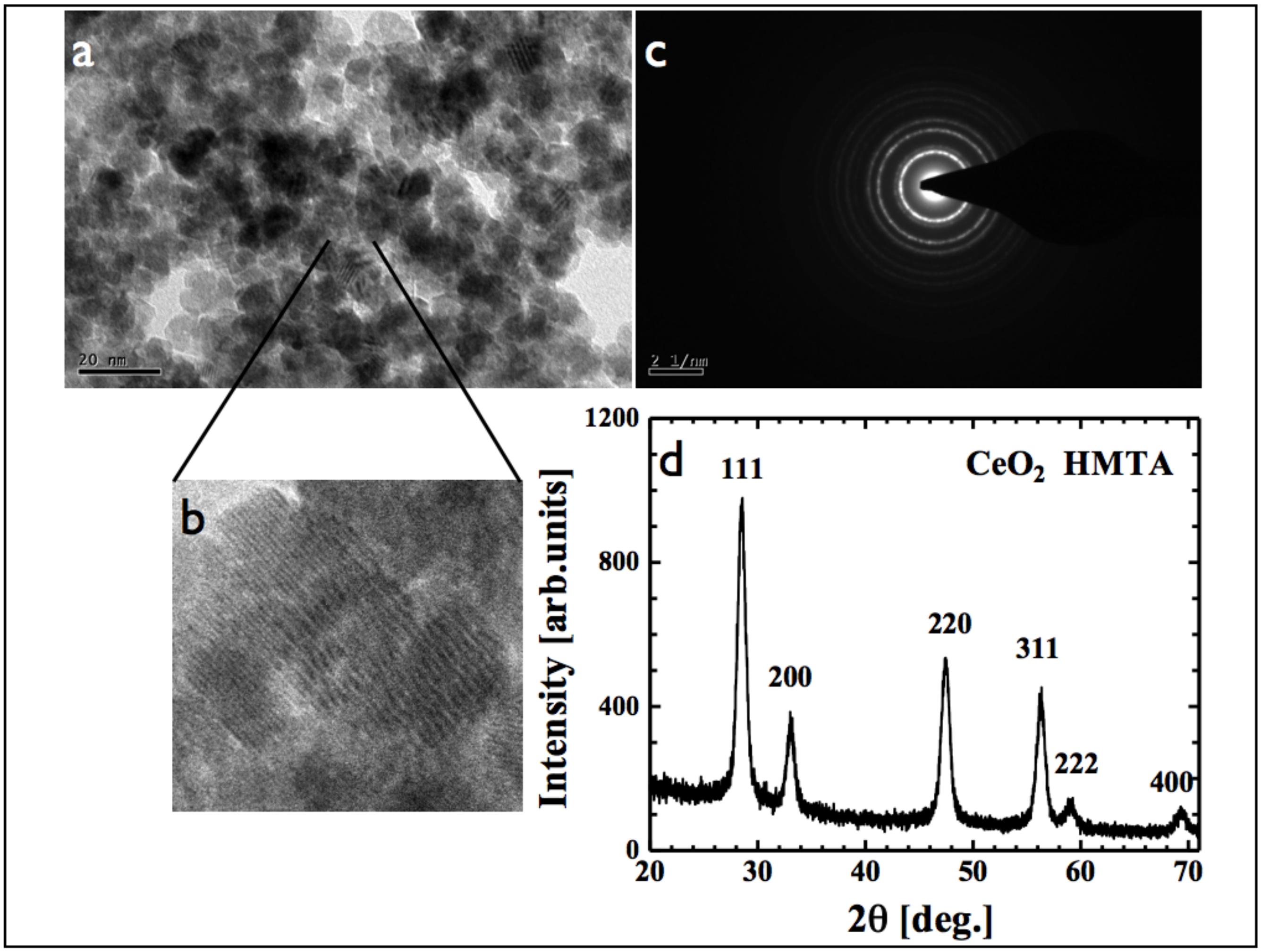

Figure S3. Characterization of the Cerium oxide nanoparticles. a, b. TEM images of the Cerium oxide nanoparticles. The outset showing the distinct fringe lines. c. Specific area electron diffraction map of cerium oxide nanoparticles d. XRD pattern of the synthesized cerium oxide nanoparticle which was found to be consistent with JCPDS no. 81-0792, and corresponds to Cerium oxide in face centered cubic phase. The peaks obtained at 2θ 28.6, 33.2, 47.8, 56.7, 69.5 and 79.7 can be indexed to 111, 200, 220, 311, 400 and 420 planes respectively. In our earlier work too we observed the similar pattern[18,19].

Synthesis and characterization of graphene oxide:

Graphene oxide was synthesized from Tassar silk cocoon as described earlier by our group[20]. Tasar silk cocoon were grounded to fine powder in pestle and mortar. This fine powder was pyrolyzed in argon (Ar) atmosphere in a muffle furnace (400 °C, 2 h). Formation of a black colored powder was observed, which was further purified by washing with ether and acetone in a soxhlet. This was further subjected to oxidation by treatment through concentrated nitric acid for 24 hours. Color change from black to brown was observed. Further washing was done to remove the residual acid. Brown powder thus obtained was vacuum dried and characterized. The sample was further characterized by XRD and Raman spectroscopy analysis, and is in agreement with the previously reported results.

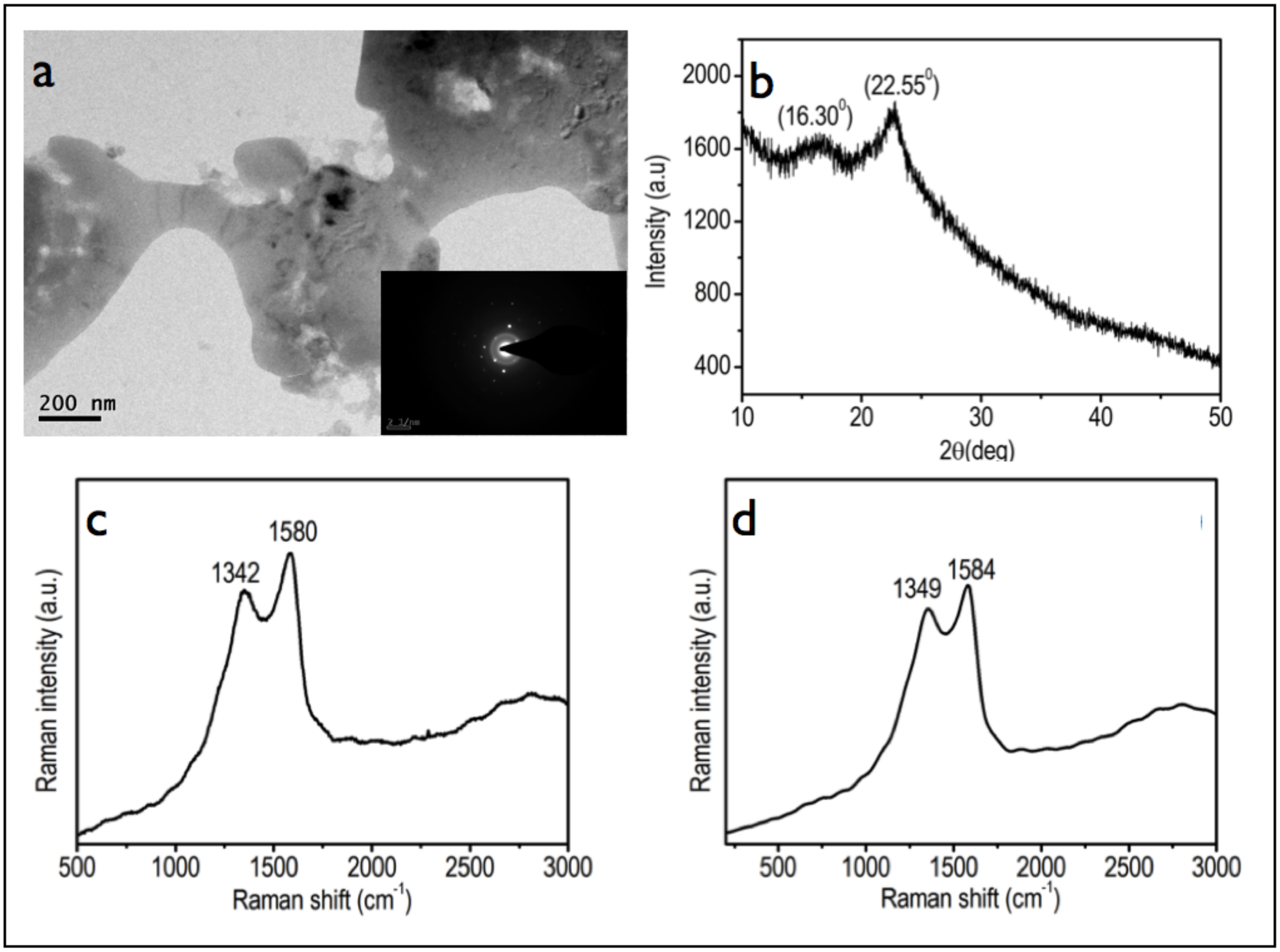

Figure S4. Characterization of the graphene oxide nanomaterial derived from Tassar silk cocoon. a. TEM image of the material. The inset shows the selected area electron diffraction map. b. The structural characterization of oxidized soot was done by powder XRD technique. In the powder XRD of nitric acid treated purified soot, the peaks at $2\theta = 16.30^0$ and 22.55^0 corresponds to the d spacing to 5.43Å and 3.92 Å respectively. The higher d-spacing 5.43Å occurs due to interlayer spacing between graphene oxide sheets. The peak d spacing around 3.92 Å attributed to the stacking of disordered graphene sheets of non oxidized shoot. The powder XRD pattern of graphene oxide depends on the presence of hydroxyl and carboxylic acid group anchored on the surface of oxidized soot after oxidation process. These hetero atoms are responsible for such in the peak positions[20-23]. c, d. Raman spectra of raw carbon soot (c) and graphene oxide derived from silk (d). The Raman spectrum of raw carbon shows two intense peak around 1580 cm^{-1} and 1342 cm$^{-1.}$ The band centered at 1580cm^{-1} is attributed due to G-band and 1342 cm^{-1} corresponds to disordered induced mode of graphite. The Raman spectra of oxidized shoot shown in figure (d) clearly indicated that there is slight shift of both the G and D band towards higher wave number. The G band for oxidized shoot is centered at 1584 cm-1 where as D band is obtained at 1349 cm^{-1}. From the figure it is clearly seen that there is a increase of D-line as compared to G-line due to introduction of Sp3 hybrdised carboxylic acid and hydroxyl group on the surface of raw shoot. Such type chemical doping also responsible for blue shift of both G and D band of oxidized shoot[20,24].

References:

1. L. E. Gregory, *Amer. J. Bot.*, 1981, **68**, 586-588.

2. M. J. O. a. O. O. P. Olatunji D., *African Journal of Plant Science*, 2013, **7**, 325-330.

3. V. Purohit, L. M. S. Palni and S. Nandi, *Physiol Mol Biol Plants*, 2009, **15**, 319-326.

4. A. H. H. a. H. J. Luippold, *Plant Physiol.* , 1960, **35**, 486-494.

5. A. H. Henry L. Speer, and William Vidaver, *Plant Physiol.* , 1974, **54**, 852-854.

6. C. YJ, *China Biogas 4:34–35*, (1999)

7. A. M. a. A. Shabrangi, Progress In Electromagnetics Research Symposium, Beijing, China, 2009.

8. G. A. Morozov, V. I. Blokhin, N. E. Stakhova, O. G. Morozov, N. V. Dorogov and A. S. Bizyakin, *World Journal of Agricultural Research*, 2013, **1**, 39-43.

9. Q. Wang, G. Chen, H. Yersaiyiti, Y. Liu, J. Cui, C. Wu, Y. Zhang and X. He, *PLoS ONE*, 2012, **7**, e47204.

10. S. A. M. a. F. T. Maryam Yaldagard, *Afr. J. Biotechnol.*, 2007, **7**, 2465-2471.

11. B. L. Aliero, *African Journal of Biotechnology*, 2004, **3**, 179-181.

12. M. O. Offiong, Udofia, S. I., Olajide, O. and Ufot, I. N., *African research review*, 2010, **4**, 368-378.

13. G. Srivastava, A. Das, T. S. Kusurkar, M. Roy, S. Airan, R. K. Sharma, S. K. Singh, S. Sarkar and M. Das, *Mater. Express*, 2014, **4**, 23-31.

14. O. Fontaine, C. Huault, N. Pavis, J. P. Billard, Plant Physiol Biochem, 1994, **32**, 677-83.

15. L. S. Katzman, A. G. Taylor, R. W. Langhans, Hort Sci, 2001, **36**, 979-81.

16. M. Zeinalabedini, K. Majourhat, J. A. Hernández, P. Martínez-Gómez, Seed Sci Technol, 2009, **37**, 267-75.

17. G. Barba-Espin, P. Diaz-Vivancos, M. J. Clemente-Moreno, A. Albacete, L. Faize, M. Faize, et al. Plant Cell Environ, 2010, **33**, 981-94.

18. S. K. Ujjain, A. Das, G. Srivastava, P. Ahuja, M. Roy, A. Arya, K. Bhargava, N Sethy, S. K. Singh, R. K. Sharma, M. Das, *Biointerphases*, 2014, **9**, 031011.

19. A. Arya, N. K. Sethy, S. K. Singh, M. Das, K. Bhargava, *Int J Nanomedicine*. 2013, **8**, 4507-20.

20. M. Roy, T. S. Kusurkar, S. K. Maurya, S. K. Meena, S. K. Singh, N. K. Sethy, K. Bhargava, R. K. Sharma, D. Goswami, S. Sarkar, M. Das, *3 Biotech*, 2014, **4** , 67-75

21. D. C. Marcano, D. V. Kosynkin, J. M. Berlin, A. Sinitskii, Z. Sun, A. Slesarev, L. B. Alemany, Lu, W, J. M. Tour, ACS nano, 2010, **4**, 4806-4814.

22. Y. Wu, B. Wang, Y. Ma, Y. Huang, N, Li, F. Zhang, Y. Chen, *Nano Res.* 2010, **3** , 661-669.

23. M. Saxena, S. Sarkar, RSC Advances, 2014, **57**, 30162-30167

24. A. Ferrari, J. Meyer, V. Scardaci, C. Casiraghi, M. Lazzeri, F. Mauri, S. Piscanec, D. Jiang, K. Novoselov, S. Roth, Phys. Rev. Lett. 2006, **97**, 187401.